Geotectonics, Vol.33, No. 5, 1999, pp. 386–398. Translated from Geotektonika, No. 5, 1999, pp. 52–66.


# Stratigraphic and Tectonic Setting of the Olistostromal Flysch Complex, Western Aleutian Basin Coast, Northern Kamchatka Peninsula

**N. A. Bogdanov[1], J. I. Garver[2], D. V. Chekhovich[1], T. N. Palechek[1], G. V. Ledneva[1], A. V. Solov'ev[1], and D. V. Kovalenko[1]**

[1] *Institute of the Lithosphere of Marginal Seas, Russian Academy of Sciences, Staromonetnyi per. 22, Moscow, 109180 Russia*

[2] *Geology Department, Olin Center, Union College, Schenectady, New York, 12308 USA*

Received December 22, 1997

**Abstract**—New data on the age and geochemistry of the sedimentary matrix and olistoliths from the olistostromal flysch complex of the western Aleutian basin coast are discussed. The aleuropelitic members of the olistostromal flysch and Ukelayat flysch complexes are similar in composition. This indicates their formation in the same basin. Based on the comprehensive analysis of the new data, new geodynamic models are proposed for the evolution of the western Bering Sea coast.

## INTRODUCTION

A new complex at the western Bering Sea coast between Amayan and Glubokaya Bays (northeastern Olyutorsky zone, Koryak Highlands) was first described in 1980. This complex was interpreted as an oceanic olistostrome because its terrigenous matrix composed of flysch facies was found to be of deep-sea origin, and numerous olistoliths of oceanic-type basalts and siliceous rocks were documented [4].

The belt of olistostromal flysch members trends northeastward along the Aleutian Basin coast no farther than Anastasia Bay. To the north, the region is composed of the flysch members of the Ukelayat zone, which underlie the complexes of the Olyutorsky zone obducted along the Vatyna-Vyvenka thrust. In the southern frontal Olyutorsky zone, olistostromes were also distinguished beneath the Vatyna-Vyvenka thrust [1, 9, 10].

The aim of this study was to reconstruct the provenance area of the terrigenous material for the olistostromal flysch complex, elucidate the origin of the olistoliths, and date the rocks of the complex. Based on the comparative analysis of the compositions of the olistostromal flysch and Ukelayat flysch complexes, a possible geodynamic setting was reconstructed, and a principal formational model was proposed for the flysch members of the northwestern Bering Sea framing.

## GEOLOGIC SETTING

The Olyutorsky tectonic zone, a constituent of the folded Bering Sea framing, occupies the southern Koryak Highlands. The complexes of the Olyutorsky zone are obducted onto the deposits of the Ukelayat depression along the Vatyna-Vyvenka thrust [9], the Ukelayat depression separating the Olyutorsky zone from the more northern accretionary complexes of the central Koryak Highlands [12]. The Olyutorsky Ridge is located in the eastern part of the Olyutorsky zone and borders the structures of the deep-sea Aleutian Basin in the east. The Olyutorsky Ridge is composed of Late Cretaceous–Paleogene volcanogenic, siliceous, and clastic rocks of oceanic and island-arc types [2-4, 16]. These deposits are deformed and make up a complex package of allochthonous nappes.

The Olyutorsky Ridge structures trend southwest-northeast. In the Anastasia Bay and Matysken River valley areas, the folds of the Ukelayat zone are oriented sublongitudinally. Relationships between the Ukelayat flysch and olistostromal flysch complexes are unknown.

The olistostromal flysch complex is the structurally and hypsometrically lowest tectonic unit on the eastern slope of the Olyutorsky Ridge. This complex is overlain by the subhorizontal isolated or fault-separated allochthonous nappes of Senonian cherts and island-arc volcanics (Fig. 1) [3, 4, 16].

## STRUCTURE OF THE OLISTOSTROMAL FLYSCH COMPLEX

The olistostromal flysch complex can be divided into olistostromal and flyschoid sequences. The *olistostromal* sequence is composed of terrigenous matrix (siltstones and mudstones interbedded with subordinate sandstones) containing small (5–10 cm) and large (0.5-5 m) olistoliths of mainly pillow basalts with hyaloclastites and cherts. On the eastern coast of Cape

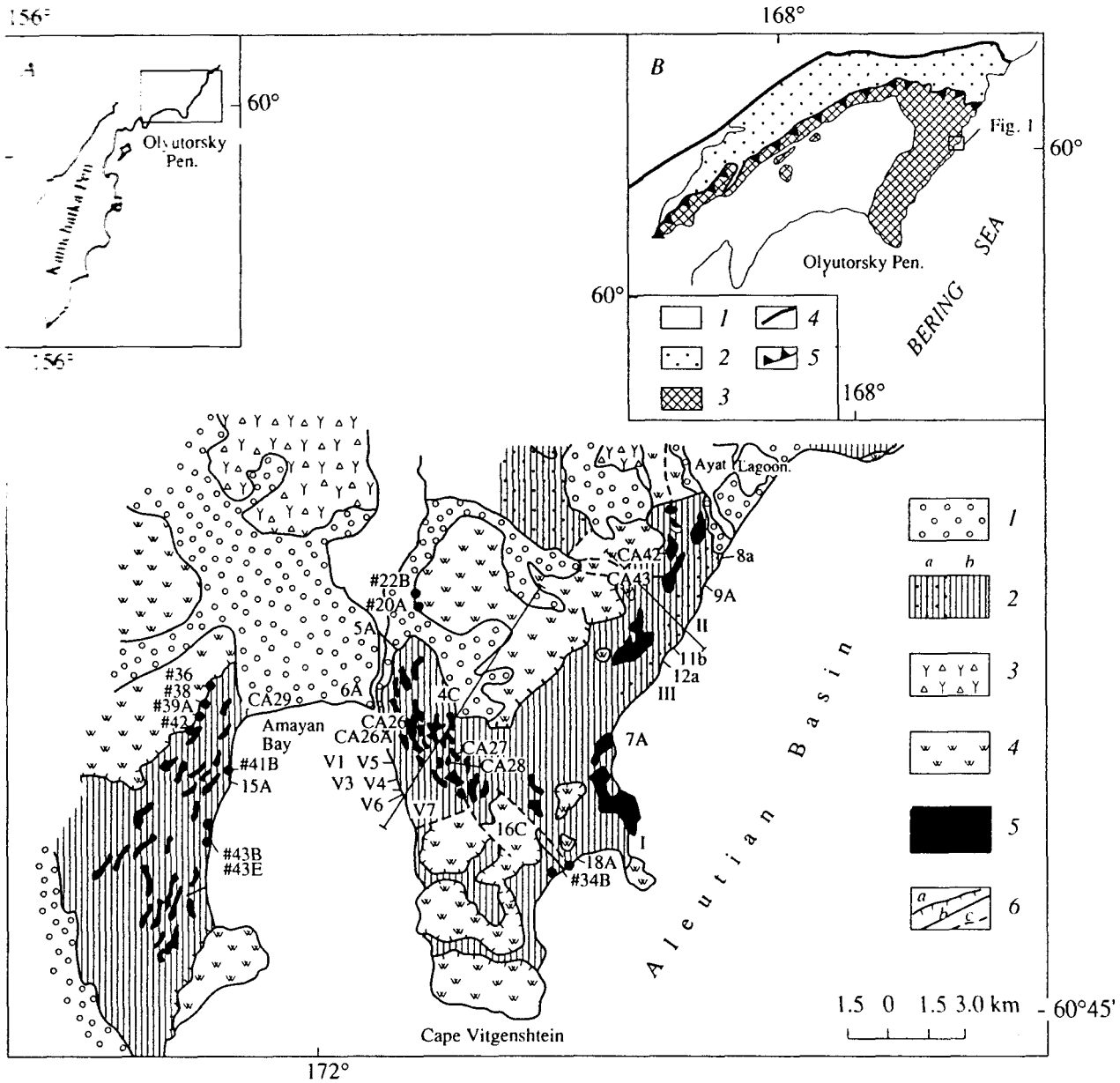


Fig. 1. Geological structure of the Aleutian Basin coast (the Amayan–Glubokaya Bay area). Location maps of the region concerned and of the study area within the southern Koryak Highlands (the Olyutorsky and Ukelayat zones) are shown in the insets *A* and *B*, respectively. (*1*) Quaternary deposits: (2) Campanian-Paleogene olistostromal flysch complex; (*3–4*) allochthonous nappes of the Senonian calcalkaline volcanics [4] *(3)* and Campanian–Maastrichtian siliceous rocks *(4): (5)* olistoliths of basalts with hyaloclastites; (6) faults: *(a)* thrusts and *(b, c)* steeply dipping faults: *(b)* proved and (c) inferred. Filled circles mark samples dated by radiolarian assemblages: points and numerals indicate samples, for which geochemical analyses were made. Inset *B: (I)* Cenozoic deposits; (2) Cretaceous-Paleogene deposits of the Ukelayat zone; *(3)* Cretaceous-Paleogene complexes of the Olyutorsky zone; *(4)* northern boundary of the Ukelayat zone; *(5)* Vatyna-Vyvenka thrust.

Vitgenshtein, we found a basalt lava flow having chilled contacts with clastic rocks.

The olistostromal sequence is characterized by the presence of flow folds, creeping structures, and traces of olistolith displacements in the matrix, which presumably had resulted from movements of exotic blocks in partially consolidated sediment. These syngenetic structures prove the olistostromal origin of the sequence.

The relatively more solid rocks (sandstones) of the terrigenous matrix of the olistostrome are fragmented and also displaced along with the exotic olistoliths. The sandstone beds have a boudinage structure. The siltstones and mudstones show traces of tectonic flow and occur between the boudines. The sequence is strongly cleavaged. Crush zones border shear faults that resulted from compression subparallel to the bedding planes. Thrusts of different classes (from a few centimeters to

hundreds of meters) produced a complicated imbricate structure at different hierarchical levels. The rock slices generally dip northwest.

The uniform deformation of the olistoliths and the matrix, their contemporaneous displacements, as well as the uniform orientation of the bedding and cleavage in the olistoliths and matrix suggest that the olistostromal sequence existed as a single unit since the time of its origin. This suggests that this sequence originated as an olistostrome that later experienced deformation and locally transformed into a tectonic melange.

The *flyschoid* sequence is composed of mudstones, siltstones, and sandstones with subordinate olistoliths and is characterized by distinct rhythms. This sequence is less tectonized. The clastic rocks are deformed to isoclinal folds of southern and southeastern vergences. The axial planes of folds are cleavaged. The southern limbs of the folds with hinges dipping steeply north-northwest are commonly tectonically displaced, thus forming a complicated thrust folds structure.

Relationships between the sequences are not quite clear. The olistostromal sequence seems to have been thrust over the flyschoid one.

## COMPOSITION OF THE OLISTOSTROMAL FLYSCH COMPLEX

The concentrations of all trace elements were determined by inductively coupled plasma mass spectrometry (ICP/MS) in a laboratory of the Geology Department, Union College, Schenectady, NY, USA. All samples were prepared using an acid dissolution method. Element concentrations in the natural samples were computed from two analyses. The analytical precision was determined using the NBS-688 (basalt) and NBS-278 (obsidian) international standards. The errors were less than 2-3%.

### *Clastic Rocks from the Olistostromal Flysch Complex*

**Mudstones and siltstoness** from the flyschoid sequence are high in V, Sr, and Zr and low in Cr and Ni (Table 1). They show Cr/Ni values of 1.1-2.3 (1.7, on the average), V/Cr values of 2.0-3.2 (2.5, on the average); and V/Ni values of 2.5-5.5 (4.5, on the average). These rocks are enriched in LREE relative to MREE and HREE and show a positive Ce anomaly (Ce/Ce* = 1.05, average of 5 determinations) and a negative Eu anomaly (Eu/Eu* = 0.72, average of 5 determinations) (Fig. 2, *B,* C, *E, F*). The mudstones and siltstones from the olistostromal sequence are similargeochemically to those from the flyschoid sequence. They are also enriched in Sr and Zr and show average Cr/Ni values of 1.4, average V/Cr values of 1.9and average V/Ni values of 2.87. They are also more enriched in LREE than in MREE and HREE and show a poorly expressed Ce and a distinct Eu anomaly.

**Sandstones** from both sequences are composed of quartz, feldspar, volcanic clasts, namely, volcanic glass, and usually contain muscovite and single grains of garnet.

The mudstones and siltstones from both sequences show Cr/Ni ratios, which are characteristic of ultramafics (~1.2–1.6), but the low contents of these elements (Table 1) indicate that muddy–silty rocks from the olistostromal flysch complex are poor in ultramafic material. Taking into account the high Sr and Zr concentrations in feldspars and zircons, respectively, it can be suggested that the muddy-silty rocks of Cape Vitgenshtein accumulated as a result of the erosion of the basement of an ensialic island arc or a continental margin [20]. The REE distributions in the mudstones and siltstones from both sequences of the olistostromal flysch complex are comparable with those in rocks that experienced differentiation in the crust. The values of REE normalized to the post-Archean Australian Schist (PAAS), almost equal to one, and the presence of volcanic clasts in the sandstones indicate that the material was removed by the erosion of an active continental margin.

### *Comparison of the Compositions of Clastic Rocks from the Olistostromal Flysch and Ukelayat Flysch Complexes*

The aleuropelites from the matrix of the olistostromal flysch and Ukelayat flysch complexes show similar distribution patterns of REE and other trace elements (Figs. 2*A*, 2*D*), but the former are characterized by lower Cr/Ni and V/Cr ratios. The aleuropelites from the Ukelayat flysch have Cr/Ni and V/Cr values of 2.9 and 10.6 in the Il'pivayam River area, and values of 2.5 and 9.4 in the Matysken River area, respectively. This suggests that the terrigenous material accumulated owing to the erosion of mainly basic volcanics and minor ultramafics. Despite the compositional difference of the aleuropelites from the olistostromal flysch and Ukelayat flysch complexes, their compositions suggest that they formed in similar environments owing to the erosion of an ensialic island arc or a continental margin.

### *Olistoliths and Basaltic Lava Flows*

**Basalts.** Basaltic bodies are abundant in the olistostromal sequence east and west of Amayan Bay. The basalts are amygdaloidal, slightly porphyritic, and aphyric. Porphyroclasts are represented by pseudomorphs of chlorite after a prismatic mineral, supposedly olivine, and in some cases by saussuritized plagioclase; the phenocrysts consist of plagioclase alone or of plagioclase and clinopyroxene. The rocks are usually spilitizied. The groundmass is composed of chlorite orof chlorite and epidote. It displays aphanitic, apointersertal, apointersertal with elements of diabasic, and minor glassy-variolitic and radiating textures. The pores are filled with carbonate alone, carbonate and chlorite, or with chlorite alone.

**Table 1.** Trace element abundances in mudstones and siltstones from the matrix of the olistostromal flysch complex of Cape Vitgenshtein and the Ukelayat flysch

| Sample no. | 4C | 5A | 6A | 7A | 15A | 16C | 18A | 8a | 9A | 11b | 12a | 03A | 03B | 03C | 03E |
|---|---|---|---|---|---|---|---|---|---|---|---|---|---|---|---|
| Elements | Olistostromal sequence | | | | | | | Flyschoid sequence | | | | Ukelayat flysch | | | |
| $TiO_2$, % | 0.86 | 0.81 | 1.10 | 1.25 | 0.97 | 0.86 | 0.90 | 1.08 | 0.94 | 1.12 | 1.50 | 1.19 | 0.98 | 0.81 | 0.91 |
| Sc, ppm | 30 | 28 | 29 | 32 | 39 | 27 | 26 | 53 | 28 | 42 | 46 | 48 | 28 | 26 | 44 |
| V | 159 | 141 | 190 | 216 | 156 | 133 | 157 | 183 | 173 | 231 | 238 | 245 | 197 | 140 | 164 |
| Cr | 76 | 97 | 96 | 111 | 83 | 66 | 78 | 100 | 87 | 94 | 9 | 19 | 89 | 77 | 82 |
| Co | 12 | 22 | 13 | 44 | 15 | 14 | 11 | 2 | 4 | 11 | 16 | 7 | 4 | 4 | 8 |
| Ni | 47 | 67 | 48 | 113 | 77 | 44 | 41 | 23 | 38 | 45 | 52 | 51 | 45 | 24 | 40 |
| Cu | 48 | 48 | 54 | 69 | 49 | 41 | 38 | 25 | 23 | 72 | 89 | 38 | 8 | 40 | 46 |
| Sr | 100 | 122 | 106 | 254 | 128 | 99 | 88 | 98 | 96 | 128 | 156 | 137 | 105 | 91 | 100 |
| Zr | 193 | 198 | 253 | 301 | 243 | 192 | 220 | 261 | 198 | 262 | 246 | 326 | 245 | 185 | 267 |
| Nb | 13 | 13 | 18 | 23 | 21 | 14 | 19 | 15 | 13 | 17 | 16 | 21 | 17 | 10 | 15 |
| Ba | 574 | 712 | 806 | 1087 | 731 | 854 | 483 | 614 | 650 | 794 | 710 | 919 | 1035 | 463 | 522 |
| Hf | 4.86 | 5.17 | 7.03 | 7.88 | 5.83 | 5.03 | 6.06 | 5.11 | 5.43 | 6.03 | 5.47 | 6.66 | 6.09 | 5.33 | 5.37 |
| Ta | 0.65 | 0.81 | 1.10 | 1.35 | 1.05 | 0.76 | 1.12 | 0.74 | 0.81 | 0.82 | 0.76 | 1.00 | 0.96 | 0.65 | 0.68 |
| Pb | 13 | 31 | 20 | 31 | 25 | 16 | 18 | 15 | 11 | 12 | 17 | 16 | 12 | 8 | 11 |
| Th | 7.39 | 9.40 | 10.16 | 14.64 | 13.77 | 8.39 | 13.74 | 7.65 | 8.59 | 8.84 | 8.41 | 10.61 | 10.29 | 6.04 | 7.15 |
| U | 2.16 | 2.21 | 2.04 | 3.52 | 2.92 | 2.21 | 2.66 | 2.63 | 2.46 | 2.69 | 2.59 | 3.46 | 3.05 | 0.47 | 2.30 |
| La | 24.73 | 27.79 | 39.42 | 50.05 | 43.25 | 3.86 | 43.70 | 26.88 | 28.32 | 25.68 | 25.14 | 38.00 | 45.41 | 22.45 | 16.31 |
| Ce | 53.50 | 58.53 | 80.55 | 100.42 | 89.00 | 63.19 | 86.37 | 57.57 | 6.16 | 52.21 | 57.72 | 79.08 | 89.70 | 47.75 | 35.11 |
| Pr | 6.33 | 6.86 | 9.97 | 12.12 | 9.98 | 7.39 | 9.98 | 6.38 | 6.75 | 6.05 | 6.77 | 8.75 | 10.21 | 5.82 | 4.05 |
| Nd | 26.18 | 27.54 | 40.21 | 48.29 | 40.15 | 28.99 | 38.92 | 25.70 | 26.70 | 24.95 | 28.37 | 35.13 | 38.80 | 23.89 | 18.80 |
| Sm | 5.24 | 9.21 | 8.47 | 9.04 | 7.39 | 5.34 | 6.86 | 4.31 | 4.83 | 4.91 | 5.67 | 6.24 | 6.17 | 4.57 | 3.72 |
| Eu | 1.20 | 1.85 | 3.10 | 3.00 | 1.49 | 1.13 | 1.87 | 0.76 | 1.17 | 1.16 | 1.31 | 1.30 | 1.87 | 1.19 | 0.81 |
| Gd | 4.81 | 4.81 | 8.18 | 7.98 | 7.02 | 4.96 | 6.73 | 3.45 | 3.93 | 4.87 | 5.40 | 5.69 | 5.46 | 3.87 | 3.90 |
| Tb | 0.74 | 0.87 | 1.31 | 1.34 | 1.03 | 0.74 | 1.05 | 0.53 | 0.65 | 0.77 | 0.86 | 0.81 | 0.83 | 0.26 | 0.61 |
| Dy | 4.38 | 4.67 | 7.15 | 6.99 | 6.04 | 4.29 | 5.74 | 3.71 | 4.39 | 4.97 | 5.06 | 5.02 | 5.03 | 3.82 | 3.86 |
| Ho | 0.89 | 1.03 | 1.64 | 1.76 | 1.21 | 0.90 | 1.25 | 0.79 | 0.98 | 1.30 | 1.05 | 1.10 | 1.12 | 0.56 | 0.83 |
| Er | 2.59 | 2.82 | 4.20 | 4.43 | 3.44 | 2.57 | 3.32 | 2.58 | 2.84 | 3.21 | 3.09 | 3.60 | 3.32 | 2.35 | 2.69 |
| Tm | 0.36 | 0.29 | 0.02 | 0.13 | 0.49 | 0.38 | 0.28 | 0.36 | 0.30 | 0.46 | 0.42 | 0.51 | 0.11 | 0.02 | 0.36 |
| Yb | 2.47 | 2.94 | 4.27 | 4.62 | 3.26 | 2.52 | 3.26 | 2.59 | 2.90 | 3.20 | 2.99 | 3.74 | 3.46 | 2.40 | 2.70 |
| Lu | 0.40 | 0.34 | 0.10 | 0.26 | 0.50 | 0.40 | 0.32 | 0.39 | 0.33 | 0.49 | 0.45 | 0.57 | 0.19 | n.f. | 0.38 |

Note: The letters n.f. denote contents below the analytical error. The locations of the sample sites are shown in Fig. 1.

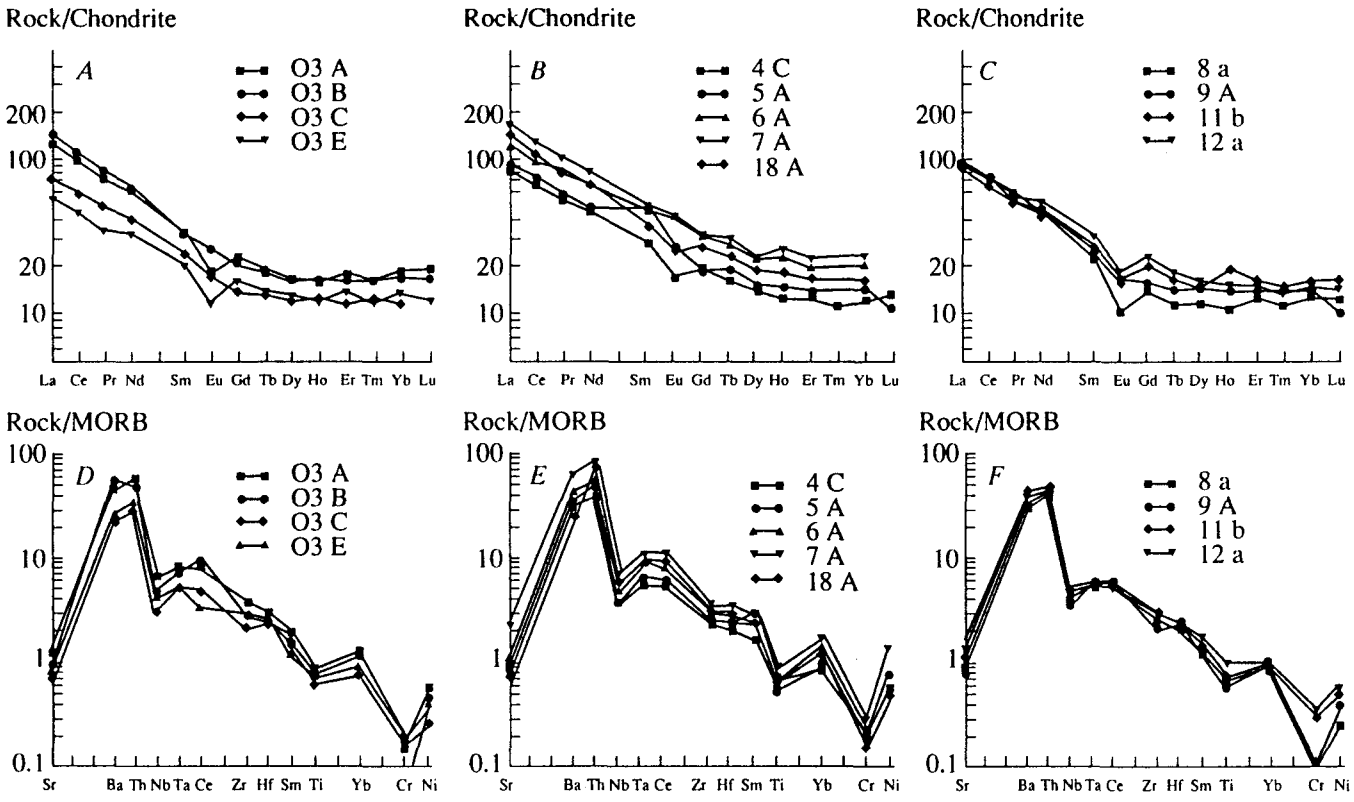


Fig. 2. Distribution of REE and other trace elements in siltstones and mudstones from the olistostromal flysch complex of Cape Vitgenshtein and the Ukelayat flysch. *(A. D)* Ukelayat flysch; *(B, E)* olistostromal and *(C, F)* fiyschoid sequences of the olistostromal flysch complex.

In accordance with the distribution of major and trace elements, two groups of basalts were identified (Table 2, Figs. 3*A*–3*D*). The first-type basalts collected from olistoliths are strongly differentiated rocks (FeO/MgO = 1.9-2.3) moderately abundant in $Al_2O_3$ (14.5 wt. %) and $K_2O$ (less than 1 wt. %) [3]. The high contents of LREE ($(La)_N$ = 58.2-81.0) at the ratios of $(La/Yb)_N$ = 3.1-5.0) (Fig. 3*B*), the elevated concentrations of high field-strength elements (HFSE), particularly, $TiO_2$ (2.13–3.70 wt. %,), Zr (168-342 ppm), Y (27-52 ppm) and Nb (31–69 ppm), and the distributions of trace elements on the spidergrams (Fig. 3D) can be correlated with those of oceanic island basalts (OIB).

The second-type basalts were collected from a lava flow in the olistostromal flysch complex and from bodies having vague (tectonic?) contacts with the matrix. They show a slight enrichment in LREE with respect to HREE (the chondrite normalized ratio of $(La/Yb)_N$ ranges from 1.2 to 1.9), the absence or the presence of a slight positive Eu anomaly indicating plagioclase fractionation (Fig. 3*A*), the moderate contents of $TiO_2$ (1.00–1.99 wt. %), the low concentrations of Cr (209-275 ppm), Ni (61–174 ppm), and V (170–278 ppm), suggesting their significant differentiation, a slight abundance in large ion lithophile element (LILE) with respect to HFSE, and the distribution of trace elements normalized to chondrite close to one (Fig. 3*C*). These basalts resemble transitional mid-oceanic ridge basalts (T-type MORB).

**Siliceous rocks** from the olistoliths of the olistostromal flysch complex are represented by cherts, jaspers, and siliceous rocks with tuffaceous impurities. The groundmass is almost totally replaced by chlorite. The volume of clastic material is 25%. The clasts of a 0.2 mm size are composed of quartz, zoned plagioclase (mainly andesine), and subordinate feldspar, pyroxene, and chlorite presumably after volcanic glass. Single radiolarias are recrystallized and replaced by chlorite.

The siliceous rocks from the olistoliths are high in Ba (1379–1180 ppm) and low in Ni (27-236 ppm), Cu (81-146 ppm), and Zn (80–255 ppm) (Table 3). This suggests the presence of insoluble organic matter and the accumulation of these rocks in areas remote from hydrothermal sources. The spidergrams (Fig. 4*C*) show that these rocks are more enriched in LILE (except for Sr) than in HFSE, have lower contents of Nb relative to Th and Ce and Ti with respect to Sm and Y. They are more enriched in LREE than in MREE ($(La/Sm)_N$ = 2.48 and 2.35) and in HREE ($(La/Yb)_N$ = 3.95 and 5.52), show a negative Eu (Eu/Eu* = 0.66 and 0.83) anomaly, and are characterized by the lack or a slight positive Ce (Ce/Ce* = 1.02 and 1.18) anomaly (Table 3, Fig. 4*A*). The distributions of REE and other trace elements in

**Table 2.** Trace element abundances in basalts from the olistostromal flysch complex of Cape Vitgenshtein

| Elements | V1 | V5 | V6 | V7 | CA29 | CA26 | CA26A | CA27 | CA28 | CA42 | CA43 | V3 | V4 |
|---|---|---|---|---|---|---|---|---|---|---|---|---|---|
| $TiO_2$, % | 1.40 | 1.31 | 1.34 | 1.99 | 1.00 | 2.19 | 2.15 | 2.13 | 2.21 | 3.50 | 3.70 | 2.59 | 2.50 |
| V, ppm | 226 | 219 | 218 | 279 | 170 | 325 | 312 | 306 | 317 | 338 | 455 | 363 | 339 |
| Cr | 250 | 240 | 238 | 275 | 209 | 127 | 123 | 125 | 129 | 3 | 14 | 180 | 180 |
| Co | 43 | 38 | 37 | 60 | 34 | 38 | 38 | 39 | 42 | 31 | 37 | 41 | 41 |
| Ni | 104 | 102 | 61 | 174 | 67 | 53 | 51 | 60 | 68 | 21 | 31 | 98 | 113 |
| Cu | 98 | 93 | 77 | 64 | 68 | 57 | 54 | 53 | 56 | 21 | 51 | 57 | 46 |
| Rb | 1 | 5 | 6 | 7 | 16 | 1 | 5 | 6 | 1 | 1 | 2 | 2 | 1 |
| Sr | 96 | 341 | 230 | 208 | 545 | 249 | 270 | 409 | 575 | 120 | 213 | 256 | 221 |
| Y | 23 | 22 | 23 | 32 | 16 | 28 | 27 | 27 | 28 | 52 | 48 | 42 | 40 |
| Zr | 86 | 79 | 79 | 147 | 61 | 175 | 173 | 168 | 171 | 342 | 312 | 240 | 231 |
| Nb | 6 | 5 | 5 | 14 | 4 | 37 | 37 | 35 | 36 | 68 | 47 | 32 | 31 |
| Ba | 63 | 142 | 105 | 234 | 415 | 151 | 140 | 402 | 103 | 225 | 169 | 88 | 71 |
| La | 4.43 | 3.54 | 3.82 | 8.34 | 3.11 | 18.10 | 18.03 | 18.10 | 18.76 | 32.82 | 25.11 | 18.96 | 17.02 |
| Ce | 11.69 | 10.00 | 10.33 | 22.09 | 8.28 | 37.35 | 40.34 | 39.01 | 41.00 | 73.47 | 58.84 | 43.95 | 40.35 |
| Pr | 1.85 | 1.63 | 1.72 | 3.26 | 1.31 | 4.33 | 5.19 | 5.04 | 5.22 | 9.47 | 27.81 | 5.95 | 5.53 |
| Nd | 10.11 | 8.78 | 9.07 | 16.32 | 7.10 | 16.76 | 22.82 | 22.00 | 23.02 | 41.90 | 35.85 | 7.51 | 25.60 |
| Sm | 2.97 | 2.68 | 2.77 | 4.35 | 2.08 | 3.00 | 4.86 | 4.85 | 4.87 | 9.03 | 8.19 | 6.43 | 6.09 |
| Eu | 1.08 | 0.94 | 1.04 | 1.45 | 0.84 | 0.68 | 1.63 | 1.61 | 1.62 | 2.85 | 2.68 | 1.99 | 1.87 |
| Gd | 3.62 | 3.32 | 3.48 | 5.16 | 2.57 | 2.67 | 5.21 | 5.08 | 5.28 | 9.58 | 8.81 | 7.22 | 6.75 |
| Tb | 0.63 | 0.59 | 0.60 | 0.88 | 0.45 | 0.41 | 0.83 | 0.81 | 0.84 | 1.53 | 1.42 | 1.19 | 1.11 |
| Dy | 4.06 | 3.74 | 3.93 | 5.71 | 2.95 | 2.49 | 8.02 | 4.93 | 4.18 | 9.47 | 8.82 | 7.36 | 7.09 |
| Ho | 0.86 | 0.80 | 0.82 | 1.19 | 0.60 | 0.53 | 1.02 | 1.00 | 1.02 | 1.94 | 1.76 | 1.56 | 1.47 |
| Er | 2.31 | 2.16 | 2.27 | 3.23 | 1.66 | 1.56 | 2.75 | 2.69 | 2.80 | 5.23 | 4.76 | 4.27 | 3.99 |
| Tm | 0.34 | 0.31 | 0.32 | 0.47 | 0.23 | 0.40 | 0.39 | 0.38 | 0.40 | 0.75 | 0.69 | 0.61 | 0.58 |
| Yb | 2.09 | 1.93 | 2.01 | 3.00 | 1.49 | 2.54 | 2.52 | 2.45 | 2.54 | 4.81 | 4.21 | 3.93 | 3.69 |
| Lu | 0.32 | 0.29 | 0.30 | 0.46 | 0.22 | 0.39 | 0.37 | 0.37 | 0.38 | 0.72 | 0.64 | 0.61 | 0.56 |
| Hf | 2.32 | 2.08 | 2.05 | 3.44 | 1.51 | 3.84 | 3.81 | 3.71 | 3.72 | 7.12 | 6.32 | 5.37 | 5.06 |
| Ta | 0.38 | – | 0.29 | 0.74 | 0.35 | 2.77 | 1.91 | 1.64 | 1.70 | 4.36 | 2.94 | 1.46 | 1.47 |
| Th | 0.22 | 0.20 | 0.20 | 0.58 | 0.16 | 1.63 | 1.63 | 1.58 | 1.59 | 2.88 | 1.82 | 1.49 | 1.41 |
| U | 0.08 | 0.11 | 0.16 | 0.74 | 0.11 | 0.55 | 0.56 | 0.51 | 0.53 | 0.48 | 0.71 | 0.42 | 0.30 |

Note: The dash denotes that the content is below the analytical error. Locations of the sample sites are shown in Fig. 1.

the siliceous rocks from the olistoliths are similar to those in volcanics from island arcs and active continental margins [22].

Our study revealed that the siliceous rocks from the olistoliths contained two indicator components, namely, insoluble organic remains and a clastic material, whereas impurities derived from hydrogenic, hydrothermal, or biogenic sources are insignificant.

Our data do not contain evidence on the geochemistry of olistolith siliceous rocks with significant amounts of a clastic material.

*Siliceous Rocks from Allochthonous Nappes*

In the study area, the olistostromal flysch complex is overlain by allochthonous nappes composed of siliceous rocks (Fig. 1). In comparison with the siliceous rocks from the olistoliths, those of the allochthonous nappes contain less clastic material. The percentage of clastic material does not exceed 5%. The particles are as small as 0.01 mm and consist of quartz, plagioclase, and mafic minerals. The groundmass is a very fine-grained crystalline siliceous (quartz–chalcedony) or clayey-siliceous material. The rocks from the allochthonous

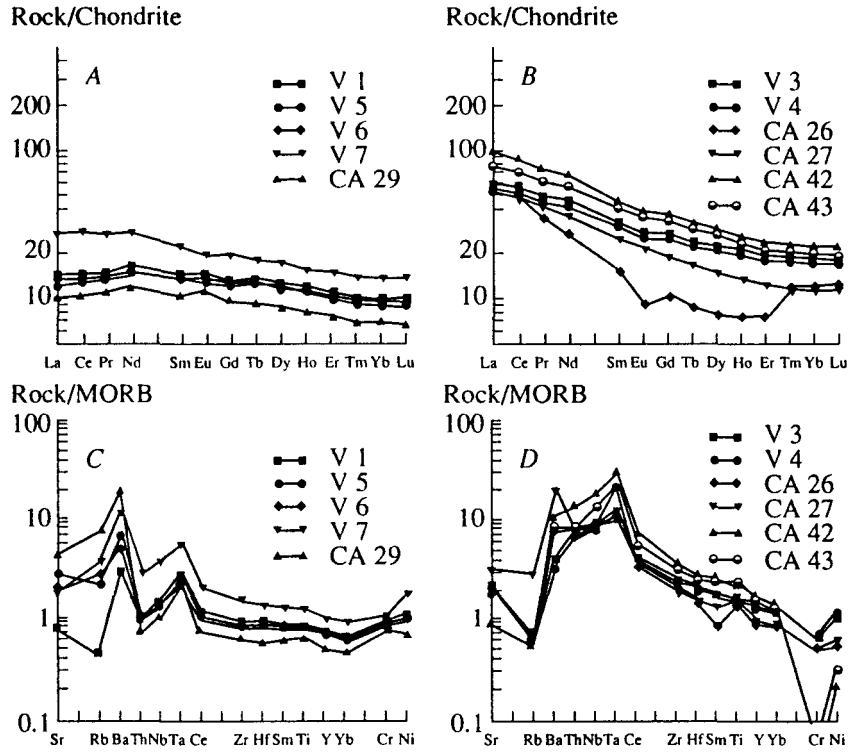


Fig. 3. Distribution of REE and other trace elements in basalts from the olistostromal flysch complex of Cape Vitgenshtein. *(A,* Q T-type MOR basalts; *(B, D)* OIB-type basalts.

nappes contain as much as 10–15% of radiolarias and sponge spicules. There are occasional brownish to brick-red jaspers with broken shells of inoceramids.

The trace element distribution in the siliceous rocks from the allochthonous nappes is similar to that in the siliceous rocks with a minor clastic material from the olistoliths (Table 3, Figs. 4*A*–4*D*). The rocks are high in Ba (681–1888 ppm), low in Ni (28–43 ppm), Cu (28-151 ppm), Zn (14–43 ppm) and $TiO_2$ (0.13–0.30 wt. %) (Table 3), and display a similar distribution of REE (Fig. 4*B*) and trace elements (with the exception of Ba and Cr) on the spidergrams. They showed the following ratio values: $(La/Yb)_N$ - 3.7-5.7, $(La/Sm)_N$ = 1.72-2.41, Eu/Eu* = 0.71–0.88, and Ce/Ce* = 1.05-1.18. These geochemical data indicate that the siliceous rocks from the allochthonous nappes and olistoliths accumulated in similar environments, except that in the former case the content of elastics was less significant.

## AGES OF THE OLISTOSTROMAL FLYSCH COMPLEX AND SILICEOUS ROCKS FROM THE ALLOCHTHONOUS NAPPES

The rocks were dated by radiolarias. Radiolarias were extracted from the siliceous rocks using the method of hydrofluoric acid dissolution and from the siltstones by boiling in hydrogen peroxide. The concentrations of the solutions and the durations of the procedures were selected experimentally. We used the methods described in [11, 21]. The photographs of radiolarias were taken by V.V. Bernard at the Institute of the Lithosphere of Marginal Seas, RAS, on an ISI-60 scanning electronic microscope.

The muddy–silty rocks from the olistostromal sequence are very poor in a microfauna. Single radiolarias with a Cenozoic habit (Fig. 5) were extracted from the matrix. The nannoplankton assemblage of a low taxonomic diversity indicated the Santonian-Maastrichtian age of the sequence [17].

The radiolarian assemblage of *Phaseliforma laxa* Pessagno, *Clatrocyclas* cf. *gravis* Vishnevskaya, *Amphipyndaxstocki* (Campbell et Clark), *Archaeodictyomitra regina* (Campbell et Clark,) *Dictyomitra densicostata* Pessagno, *Xitus asymbatos* (Foreman), *Stichomitra* aff. *compsa* Foreman, and *Theocampe* sp. (Fig. 5) indicates the Campanian-Maastrichtian age of the siliceous rocks from the olistoliths.

On the western coast of Amayan Bay, an olistolith of sealing-wax-red jaspers of a microscopic clastic-turbidite texture was found. It is important that the matrix of this jasper contains a cold-water radiolarian assemblage of Santonian-Campanian age. This radiolarian assemblage includes *Amphipyndax* ex gr. *stocki* (Campbell et Clark), *Dictyomitra* cf. *lamellicostata* Foreman. *D.* cf. *densicostata* Pessagno, and *D.* ex gr. *multicostata* Zittel. Judging by the radiolarian assemblage of *Pseudostylosphaera* cf. *tenuis* Nakaseko et Nishimura, *P.* aff. *goestlingensis* Kozur et Mostler, and *Triassocampe scalaris* Dumitrica, Kozur et Mostler (Fig. 6), the inclusions were

**Table 3.** Trace element abundances in siliceous rocks from the olistoliths of the olistostromal flysch complex of Cape Vitenshtein

| Sample no. | #43D | #43E | #43B | #22B | #39A | #36 | #41B | #34B | #38 | #20A |
|---|---|---|---|---|---|---|---|---|---|---|
| Elements | Olistoliths | | Allochthonous nappes | | | | | | | |
| $TiO_2$, % | 0.42 | 0.44 | 0.47 | 0.19 | 0.22 | 0.13 | 0.07 | 0.14 | 0.17 | 0.30 |
| V, ppm | 98 | 78 | 106 | 48 | 41 | 32 | 14 | 36 | 65 | 69 |
| Cr | 29 | 22 | 71 | 66 | 56 | 58 | 60 | 67 | 57 | 57 |
| Ni | 65 | 76 | 68 | 38 | 44 | 40 | 28 | 41 | 39 | 43 |
| Co | 24 | 30 | 58 | 8 | 8 | 9 | 4 | 7 | 10 | 11 |
| Cu | 81 | 84 | 146 | 28 | 75 | 28 | 56 | 61 | 67 | 152 |
| Zn | 80 | 120 | 255 | 41 | 48 | 28 | 14 | 27 | 29 | 44 |
| Rb | 36 | 51 | 89 | 20 | 20 | 11 | 9 | 14 | 16 | 27 |
| Sr | 203 | 147 | 180 | 69 | 84 | 63 | 91 | 85 | 74 | 169 |
| Y | 16 | 25 | 43 | 7 | 9 | 5 | 3 | 5 | 5 | 9 |
| Zr | 82 | 131 | 158 | 38 | 52 | 43 | 23 | 25 | 40 | 72 |
| Nb | 3 | 6 | 51 | 2 | 3 | 3 | 1 | 1 | 1 | 3 |
| Ba | 1379 | 1154 | 1180 | 1400 | 1636 | 1051 | 681 | 1243 | 2899 | 1889 |
| La | 15.59 | 16.47 | 33.54 | 5.40 | 7.33 | 4.51 | 2.19 | 4.53 | 4.61 | 6.31 |
| Ce | 39.74 | 37.97 | 52.15 | 13.44 | 18.72 | 11.74 | 5.37 | 10.20 | 11.92 | 16.88 |
| Pr | 4.33 | 4.82 | 21.33 | 1.51 | 2.06 | 1.23 | 0.62 | 1.17 | 1.38 | 1.98 |
| Nd | 18.15 | 20.07 | 106.11 | 6.23 | 8.91 | 5.36 | 2.57 | 5.08 | 5.76 | 8.53 |
| Sm | 3.95 | 4.41 | 54.64 | 1.50 | 2.10 | 1.18 | 0.65 | 1.19 | 1.68 | 2.15 |
| Eu | 1.04 | 0.96 | 30.87 | 0.35 | 0.48 | 0.26 | 0.15 | 0.30 | 0.43 | 0.56 |
| Gd | 3.64 | 4.34 | 55.90 | 1.27 | 1.85 | 1.04 | 0.51 | 0.98 | 1.23 | 1.93 |
| Tb | 0.53 | 0.71 | 14.66 | 0.18 | 0.28 | 0.14 | 0.07 | 0.14 | 0.19 | 0.30 |
| Dy | 3.20 | 4.70 | 64.59 | 1.22 | 1.83 | 0.98 | 0.51 | 0.90 | 1.15 | 1.82 |
| Ho | 0.63 | 0.95 | 15.73 | 0.23 | 0.35 | 0.18 | 0.09 | 0.18 | 0.23 | 0.37 |
| Er | 1.84 | 2.82 | 42.42 | 0.70 | 1.04 | 0.55 | 0.30 | 0.51 | 0.64 | 1.08 |
| Tm | 0.27 | 0.42 | 14.13 | 0.08 | 0.15 | 0.06 | 0.03 | 0.07 | 0.09 | 0.16 |
| Yb | 1.90 | 2.81 | 35.36 | 0.70 | 1.14 | 0.53 | 0.32 | 0.53 | 0.64 | 1.14 |
| Lu | 0.29 | 0.46 | 13.64 | 0.09 | 0.18 | 0.07 | 0.04 | 0.08 | 0.10 | 0.18 |
| Hf | 1.95 | 3.16 | 47.77 | 0.89 | 1.16 | 0.78 | 0.44 | 0.61 | 0.84 | 1.74 |
| Ta | 0.32 | 0.41 | 12.31 | 0.20 | 0.44 | 0.13 | 0.07 | 0.08 | 0.16 | 0.32 |
| Th | 2.34 | 4.45 | 19.66 | 1.76 | 1.88 | 1.34 | 0.61 | 1.05 | 1.16 | 1.91 |

Note: Locations of the sample sites are shown in Fig. 1.

dated Middle Triassic (late Anisian–earliest Ladinian). These inclusions are certainly exotic because no rocks older than the latest Early Cretaceous are known in the siliceous sequences of the Olyutorsky ridge. Olistoliths containing the Late Triassic (late Norian–Rhaetian) radiolarian assemblage of *Canoptum triassicum* Yao, *Kojurastrum quadriradiatus* (Kozur et Mostler), *Dreyericyrtium* sp., and *Haeckelicyrtium* sp. have been described earlier from the Maastrichtian olistostromal sequence located in the middle stream of the Vyvenka River near the Vatyna–Vyvenka thrust [2].

The radiolarian assemblage of *Phaseliforma* ex gr. *carinata* Pessagno, *Spongodiscus* ex gr. *volgensis* Lipman, *Stichomitra* cf. *livermorensis* Campbell et Clark, *S.* cf. *campi* Foreman, *Clathrocyclas* ex gr. *tintinnaeformis* Campbell et Clark, *C.* aff. *diceros* Foreman, and *Xitus* ex gr. *asymbatos* Foreman (Fig. 6) dales the siliceous rocks from the allochthonous nappes Campanian–Maastrichtian, which is close to the age of the siliceous rocks from the olistoliths and of some clastic rocks from the matrix of the olistostromal flysch complex.

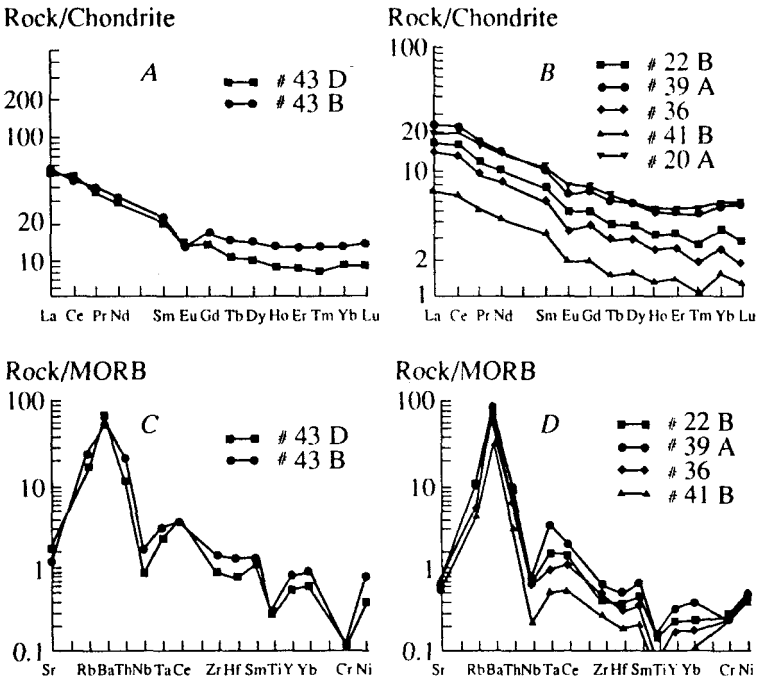


Fig. 4. Distribution of REE and other trace elements in siliceous rocks from the olistoliths of the olistostromal flyschcomplex of Cape Vitgenshtein and from allochthonous nappes overthrustonto the olistostromal sequence. *(A, C)*siliceous rocks from the olistoliths and *(B, D)* same from the allochthonous nappes.

## DISCUSSION

The similar geochemical features of the aleuropelites from the olistostromal flysch and Ukelayat flysch complexes suggest that the sequences of these two complexes accumulated in the single basin as a result of the erosion of the basement of an ensialic island arc or a continental margin. The same conclusion can be drawn from the study of the sandstones. The sandstones from the olistostromal flysch and Ukelayat flysch complexes are composed mainly of quartz, feldspar, and fragments of muscovite, and contain subordinate clasts of volcanic glass. The presence of muscovite also proves the formation of these complexes as a result of the erosion of continental rock masses.

As shown above, the terrigenous material from the Ukelayat flysch, the matrix of the olistostromal flysch complex, and the clastic material in the siliceous rocks from the allochthonous nappes and olistoliths might have originated from the same source.

Numerous bodies of OIB and T-type MOR basalts widely in the olistostromal flysch complex. We found that some T-type MOR basalt bodies had been emplaced during the sedimentation. This fact may indicate that oceanic basalts were emplaced in the area of flysch accumulation. On the other hand, the olistoliths of basalts mainly of the O1B type are as log as 1-2 km with the widths of their outcrops measuring tens to hundreds meters (Fig. 1). In general, these bodies cover about 25% of the outcrop area of the olistostromal flysch complex. This suggests that the sedimentation area of the olistostromal flysch complex was next to an interplate volcanic rise or its remnant, from which olistoliths slided by the force of gravity.

The olistostromal flysch complex formed in the Santonian-Maastrichtian time (as dated by nannoplankton) [17] and continued to accumulate in the Cenozoic (judging by the findings of the Cenozoic? radiolarias and the Eocene matrix of the complex outcroppingt in the Taman lagoon [3]). The siliceous rocks from the complex olistoliths and the cherts overlying the allochthonous nappes are almost coeval. We dated them Campanian–Maastrichtian. Previously, these rocks were dated Santonian-Danian [3]. The finding of Triassic jaspers, which are exotic to the siliceous rocks of the Olyutorsky Ridge, is evidence in support of the olistostromal origin of the complex.

## INTERPRETATION

Thus, the olistostromal flysch complex of the western Aleutian basin coast and the Ukelayat flysch accumulated most likely as a result of the erosion of the Eurasian continent rather than the ensimatic Olyutorsky arc. The rock complexes of the latter were obducted onto the flysch and constitute the central part of the Olyutorsky ridge in the present-day structure.

The Olyutorsky ridge, including the study area, is composed of lithostructural units (Fig. 1) that accumulated almost contemporaneously in various geodynamic settings [16]. These units are the olistostromal flysch complex (Campanian–Maastrichtian), marginal-sea volcano-

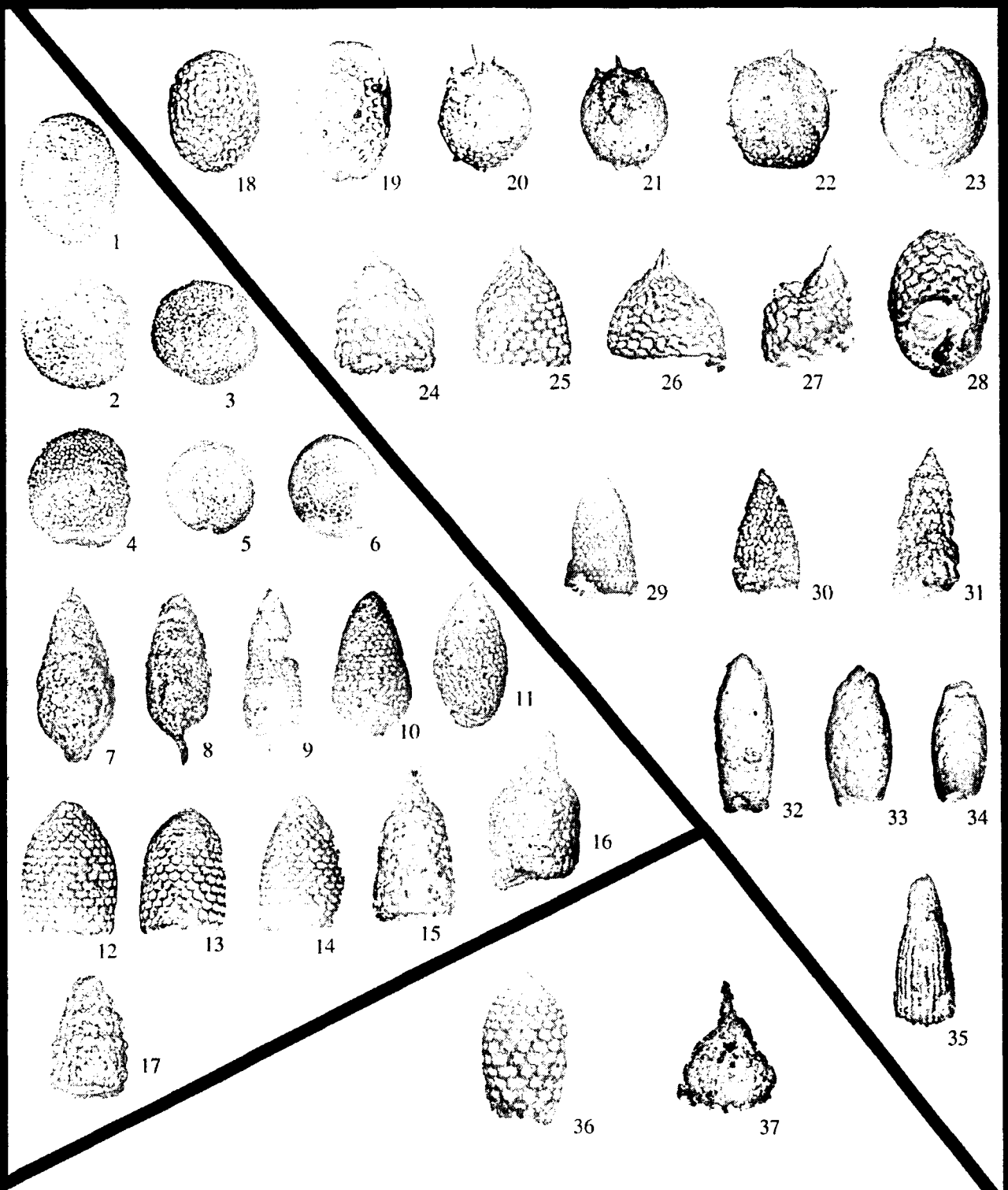


**Fig. 5.** Radiolarian assemblages from the olistostromal flysch complex from Cape Vitgenshtein. (1–17) nappes, (18–35) olistoliths, (36–37) matrix: (1) *Phaseliforma* cf. *carinata* Pessagno, ×90; (2–5) *Spongodiscus* ex gr. *volgensis* Lipman, ×100; (6) *Orbiculiforma* sp., ×100; (7–10) *Stichomitra* cf. *livermorensis* (Campbell et Clark), ×110 (7, 8, 10), ×100 (9); (11) *Stichomitra* cf. *campi* Foreman, ×100; (12–14) *Clathrocyclas* ex gr. *tintinnaeformis* Campbell et Clark, ×100; (15, 16) *Clathrocyclas* aff. *diceros* Foreman, ×100 (15), ×110 (16); (17) *Xitus* ex gr. *asymbatos* (Foreman), ×100; (18) *Phaseliforma* sp., ×100; (19) *Phaseliforma laxa* Pessagno, ×100; (20–23) *Lithomespilus* cf. *mendosa* (Krasheninnikov), ×100 (20, 21), ×110 (22, 23); (24–28) *Clathrocyclas* cf. *gravis* Vishnevskaya, ×100; (29) *Amphipyndax stocki* (Campbell et Clark), ×100; (30) *Stichomitra* aff. *compsa* Foreman, ×100; (31) *Xitus asymbatos* (Foreman), ×100; (32–34) *Theocampe* sp., ×150 (32), ×100 (33, 34); (35) *Archaeodictyomitra* cf. *regina* (Campbell et Clark), ×100; (36) *Clathrocyclas?* sp. cf. *C. universa* Clark et Campbell, ×100; (37) *Phormocyrtis?* sp., ×225.

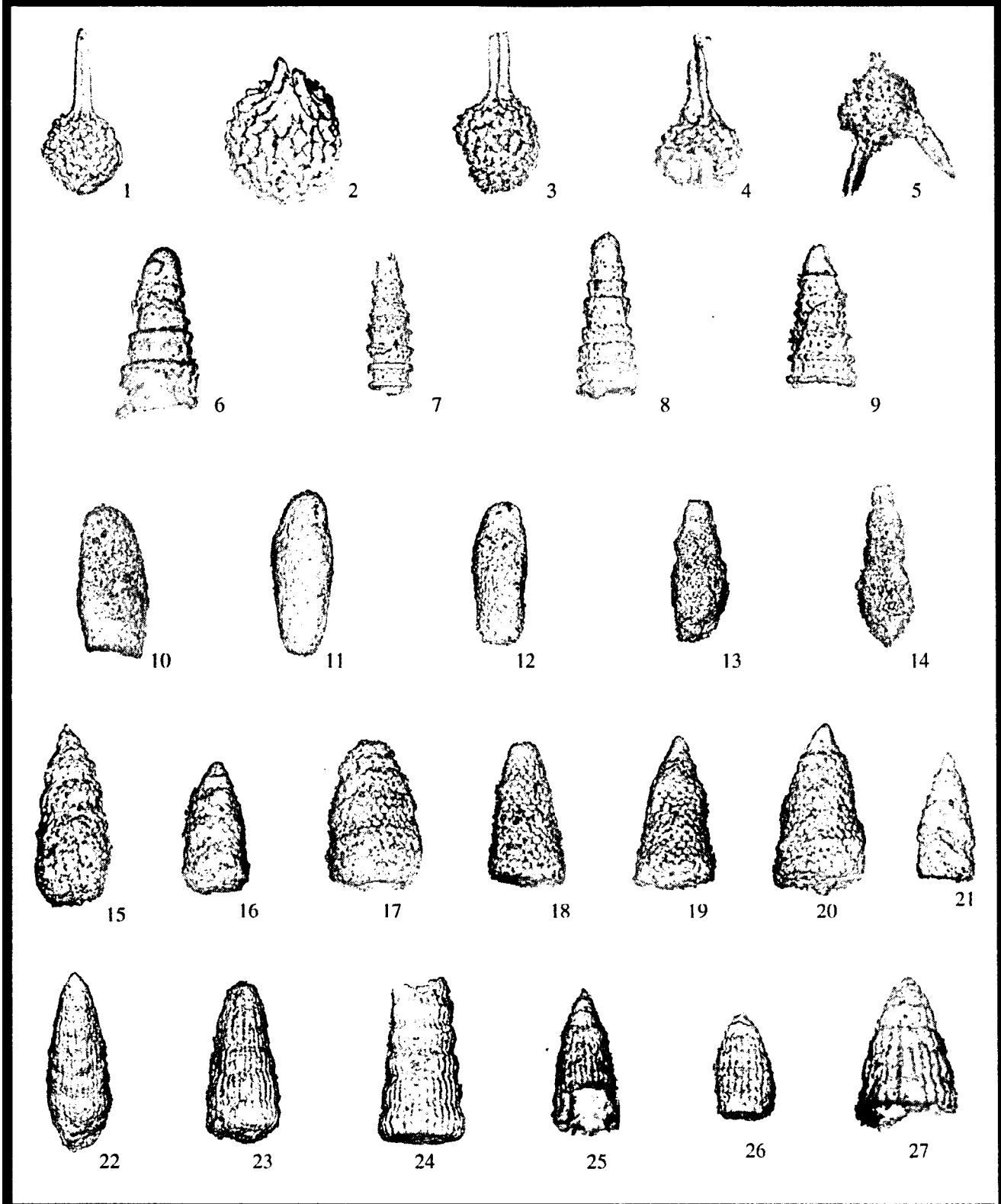


**Fig. 6.** Triassic (late Anisian–early Ladinian) radiolarian assemblage (1–9) from the inclusions in the Vatyna-type (Santonian–Campanian) matrix (10–28) from the olistostromal flysch complex of Cape Vitgenshtein.

(1–3) *Pseudostylosphaera tenuis* Nakaseko & Nishimura, ×65, ×140, ×100; (4) *Pseudostylosphaera* aff. *goestlingensis* Kozur et Mostler, ×100; (5) *Sphaerellaria* gen. et sp. indet., ×100; (6–7) *Triassocampe* cf. *scalaris* Dumitrica, Kozur et Mostler, ×150, ×80; (8–9) *Triassocampe scalaris* Dumitrica, Kozur et Mostler, ×100, ×90; (10–12) *Theocampe* sp., ×100 (10), ×90 (11), ×60 (12); (13–18) *Stichomitra sp.*, ×100 (13–15, 17, 18), ×90 (16); (19–21) *Amphipyndax* sp., ×100 (19, 20), ×90 (21); (22) *Dictyomitra* cf. *lamellicostata* Foreman, ×60; (23–27) *Dictyomitra* sp., ×100 (23, 25, 27), ×110 (24), ×90 (26).

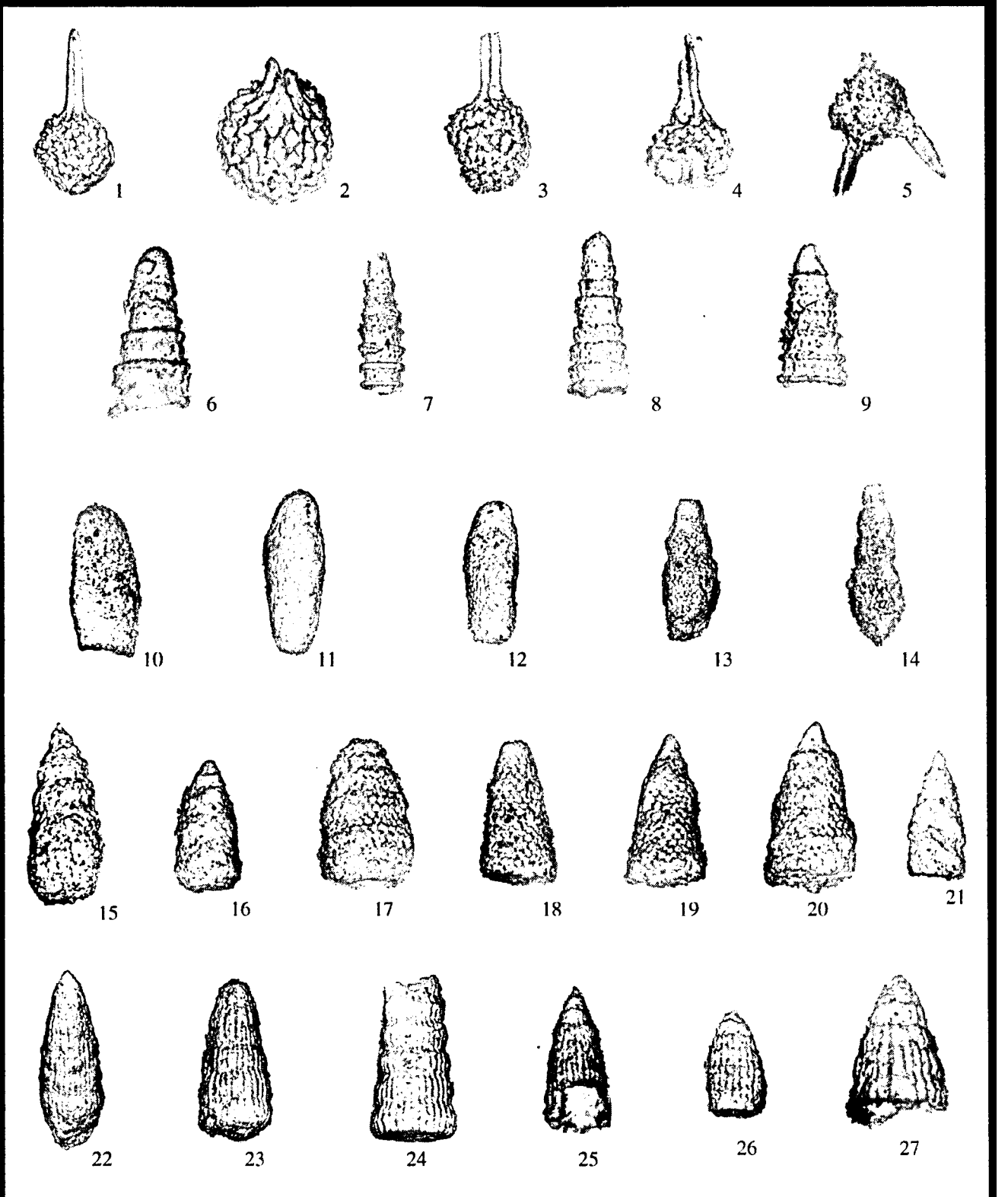


**Fig. 6.** Triassic (late Anisian–early Ladinian) radiolarian assemblage (1–9) from the inclusions in the Vatyna-type (Santonian–Campanian) matrix (10–28) from the olistostromal flysch complex of Cape Vitgenshtein.

(1–3) *Pseudostylosphaera tenuis* Nakaseko & Nishimura, ×65, ×140, ×100; (4) *Pseudostylosphaera* aff. *goestlingensis* Kozur et Mostler, ×100; (5) *Sphaerellaria* gen. et sp. indet., ×100; (6–7) *Triassocampe* cf. *scalaris* Dumitrica, Kozur et Mostler, ×150, ×80; (8–9) *Triassocampe scalaris* Dumitrica, Kozur et Mostler, ×100, ×90; (10–12) *Theocampe* sp., ×100 (10), ×90 (11), ×60 (12); (13–18) *Stichomitra sp.*, ×100 (13–15, 17, 18), ×90 (16); (19–21) *Amphipyndax* sp., ×100 (19, 20), ×90 (21); (22) *Dictyomitra* cf. *lamellicostata* Foreman, ×60; (23–27) *Dictyomitra* sp., ×100 (23, 25, 27), ×110 (24), ×90 (26).

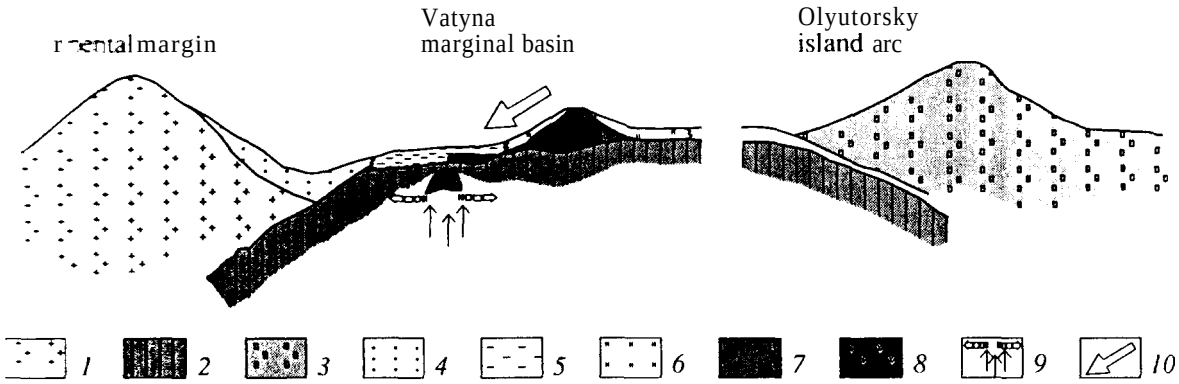


FEZ. ". Reconstructed paleolateral facies succession that existed south or southeast of the Eurasian continental margin (Koryak segment) in the late Senonian time. (*1–3*) continental *(1)*, oceanic (2) and ensimatic island-arc *(3)* types of the earth's crust; (*4–8*) areas accumulation of the Ukelayat flysch *(4)*, olistostromal flysch complex (5), cherts from the allochthonous nappes and olistoliths oceanic island basalts (7), and T-type MOR basalts of the marginal sea (*8*); *(9)* zone of the local extension and T-type MOR basalt flows: (*10*) direction of the olistolith removal into the sedimentation area of the matrix of the olistostromal flysch complex.

siliceous complex (Campanian–Maastrichtian) and island-arc sedimentary–volcanogenic complex (Campanian–Maastrichtian) [3, 14], and some members of the Ukelayat flysch (Cretaceous-Paleogene) [6]. Exactly or roughly coeval with these rocks are the cherts and subordinate elastics from the allochthonous nappes (Campanian–Maastrichtian) and rare thin chert interbeds (Campanian–Maastrichtian and Maastrichtian-Danian) associated with the subalkali OIB-type basalts, which occur in significantly smaller areas only within the study area [16].

Proceeding from the facts that these coeval lithostructural complexes are juxtaposed tectonically and occur in particular structural positions in the present-day structure and also from their geochemistries, we reconstructed a hypothetical paleolateral facies succession that had existed in the North Pacific during the Late Cretaceous.

The Ukelayat flysch is believed to have been accumulated on the Eurasian continental slope or at its base [6. 12. 15, 16]. The relationships of the Ukelayat flysch and olistostromal flysch complexes are not known. Their outcrops are separated by a 40–50-km belt of the allochthonous nappes of marginal-sea and island-arc deposits. The structural positions of these complexes, their similar geochemical features, and the significantly smaller amount of a sand material in the matrix of the olistostromal flysch complex suggest that the olistostromal flysch complex formed at a significant distance from the continent to the south or southeast from the Ukelayat flysch. The T-type MOR basalts *(in situ* flows) probably flowed through a local extension zone that existed within the sedimentation area of the olistostromal flysch complex. A volcanic oceanic rise that supplied the olistoliths of OIB-type basalts was probably located in the direct vicinity of this area.

The geochemical similarity between the siliceous rocks from the olistoliths and the aleuropelites from the Ukelayat flysch and olistostromal flysch complexes indicates that the siliceous rocks accumulated within the same basin but at a greater distance from the sedimentary provenance sources.

The marginal-sea and island-arc complexes, which are the highest structural units in the system of the tectonic nappes of the Olyutorsky ridge, seem to be the southernmost constituents of this paleolateral facies succession. This is consistent with the paleomagnetic data on the formation of the Olyutorsky arc at 50° N [7].

It can thus be concluded that a paleolateral facies succession consisting of the Eurasian continent, its continental slope and a trench, a basin with zones of local extensions and an oceanic volcanic rise, and an ensimatic island arc existed in the Koryak segment of the Eurasian continental margin in Senonian time (Fig. 7).

The later evolution of the proposed succession of the olistostromal flysch complex in the present-day structure were reconstructed from paleomagnetic [7, 8] and structural [13] studies. The flysch sequences experienced at least two deformation events. Particularly, the deformations of the first event led to the formation of the isoclinal folds of the eastern vergence; the deformations of the second event resulted in the northward overturn of the whole structure [7, 8]. The deformation of the first event is poorly known and can be ascribed to the collision of the Olyutorsky arc with the Eurasian continental margin. During the deformations of the second event, the principal axis of compression stress was oriented southeast-northwest [13]. This deformation might be caused by tectonic motions from the side of the Aleutian Basin of the Bering Sea, which resulted from back-arc spreading in the Paleogene [18].

## ACKNOWLEDGMENTS

This work was supported by the Russian Foundation for Basic Research (project nos. 93-05-9554 and 98-05-64525) and the US National Science Foundation (project nos. EAR 94-18989 and EAR 94-18990).

## REFERENCES


1. Alekseev. E.S., Evolution and Structural Features of the Southern Koryak Highland, *Geotektonika,* 1979, no. 1, pp. 85-96.
2. Astrakhantsev, O.V., Kazimirov, A.D., and Kheifets, A.M., Tectonics of the Northern Olyutorsky Zone, in *Ocherki po geologii severo-zapadnogo sektora Tikhookeanskogo tektonicheskogo poyasa* (Essays on the Geology of the Northwestern Pacific Tectonic Belt), Moscow: Nauka, 1987, pp. 161–183.
3. Bogdanov, N.A.. Vishnevskaya, V.S., Kepezhinskas, P.K., Sukhov, A.N., and Fedorchuk, A.V., *Geologiya yuga Koryakskogo nagor'ya* (Geology of the Southern Koryak Highland). Moscow: Nauka, 1987.
4. Bogdanov, N.A.. Vishnevskaya, V.S., Sukhov, A.N., Fedorchuk, A.V.. and Chekhovich, V.D., Oceanic Olistostrome on the Western Coast of the Aleutian Basin (Bering Sea), *Geotektonika,* 1982, no. 5, pp. 74-80.
5. Bogdanov, N.A.. Chekhovich, V.D., Sukhov, A.N., and Vishnevskaya, VS., Tectonics of the Olyutorsky Zone, in *Ocherki tektoniki Koryakskogo nagor'ya* (Essays on the Tectonics of the Koryak Highland), Moscow: Nauka, 1982, pp. 189-217.
6. Kazimirov, A.D.. Krylov, K.A., and Fedorov, P.I., Tectonic Evolution of Marginal Seas with Reference to the Southern Koryak Highland, in *Ocherki po geologii Severo-Zapadnogo sektora Tikhookeanskogo tektonicheskogo poyasa* (Essays on the Geology of the Northwestern Pacific Tectonic Belt), Moscow: Nauka, 1987, pp. 200–225.
7. Kovalenko, D.V. Paleomagnetism and Kinematics of the Central Olyutorsky Range, Koryak Highland, *Geotektonika,* 1996, no. 3, pp. 82-96.
8. Kovalenko, D.V.. Shcherbinina, E.I., Shikova, T.N., Solov'ev, A.V., and Pachkalov, A.S., Paleomagnetism of the Flysch-Olistostrome Sequences of the Eastern Olyutorsky Range, *Dokl. Ross. Akad. Nauk,* 1996, vol. 346, no. 3, pp. 360–363.
9. Mitrofanov, N.P.. Vatyna Nappe in the Central Koryak Fold Zone, *Geol. Geofiz.*, 1977, no. 4, pp. 144–149.
10. Mitrofanov, N.P. and Sheludchenko, S.D., The Age of Clastic Deposits in the Southwestern Central Koryak Fold Zone, *Geol. Geofiz.*, 1981, no. 4, pp. 128–131.
11. Nazarov, B.B. and Vitukhin, D.I., A Technique for Extracting Fossil Radiolaria, *Izv. Akad. Nauk SSSR, Ser. Geol.*, 1981, no. 10, pp. 95–101.
12. Sokolov, S.D., *Akkretsionnaya tektonika Koryaksko-Chukotskogo segmenta Tikhookeanskogo poyasa* (Accretionary Tectonics of the Koryak–Chukchi Segment of the Pacific Belt), Moscow: Nauka, 1992.
13. Solov'ev, A.V., Tectonic Evolution of the Flyschoid-Olistostrome Complex on the Western Coast of the Aleutian Basin, *Dokl. Ross. Akad. Nauk,* 1996, vol. 351, no. 4, pp. 513–516.
14. Solov'ev, A.V., Palechek. T.N., and Palechek, R.M., Tectonostratigraphy of the Northern Olyutorsky Zone (Koryak Highland, Anastasia Bay Area), *Stratigr. Geol. Korelyatsiya,* 1998, vol. 6, no. 4, pp. 92–105.
15. Stavskii, L.P., Chekhovich, V.D., Kononov, M.V., and Zonenshain, L.P., Palinspastic Reconstructions of the Anadyr-Koryak Region. *Geotektonika,* 1988, no. 6, pp. 32–42.
16. Chekhovich, V.D., *Tektonika i geodinamika skladchatogo obramleniya malykh okeanicheskikh basseinov* (Tectonics and Geodynamics of the Folded Rim of Minor Oceanic Basins), Moscow: Nauka, 1993.
17. Shcherbinina, E.A. and Kovalenko, D.V., The Age of the Cenozoic Flysch-Olistostrome Sequences of the Olyutorsky Range, *Stratigr. Geol. Korelyatsiya,* 1996, vol. 4, no. 2, pp. 110–112.
18. Cooper, A.K., Marlow, M.S., Scholl, P.W., and Stevenson, A.J., Evidences for Cenozoic Crustal Extension in the Bering Sea Region. *Tectonics,* 1992, vol. 11, no. 4, pp. 719-731.
19. Dymond, J., Geochemistry of Nasca Plate Surface Sediments: An Evaluation of Hydrothermal, Biogenic, Detrital, and Hydrogenous Sources, *Geol. Soc. Am. Memoir,* 1981, vol. 154, pp. 133-173.
20. Garver, J.I. and Scott, T.J., Rare Earth Elements in Argillites Indicate a Continental Provenance for Clastic Rocks in the Bridge River Complex, Southern B.C., *Geol. Soc. Am. Abstr.*, 1993, vol. 25, pp. 40–41.
21. Pessagno, E. and Newport, R.A., A Technique for Extracting Radiolaria from Radiolarian Cherts, *Micropaleontol.*, 1972, vol. 27, pp. 231–234.
22. Wilson, M., *Igneous Petrogenesis: A Global Tectonic Approach,* Boston, Sydney, Wellington: Unwin Hyman, 1989.


*Reviewers: S.D. Sokolov and A.S. Perfil'ev*